

## Unusual band dispersion in Pb films on Si(111)

M. H. Upton, T. Miller, and T.-C. Chiang

*Department of Physics, University of Illinois at Urbana-Champaign, 1110 West Green Street, Urbana, Illinois 61801-3080, USA  
and Frederick Seitz Materials Research Laboratory, University of Illinois at Urbana-Champaign, 104 South Goodwin Avenue,  
Urbana, Illinois 61801-2902, USA*

(Received 6 April 2004; revised manuscript received 7 October 2004; published 6 January 2005)

Atomically uniform Pb films are prepared on Si(111), and the quantum-well states corresponding to confined valence electrons in the film are probed by angle-resolved photoemission. The subband structure shows a free-electron-like dispersion near the zone center, but the dispersion turns sharply toward higher binding energies at larger in-plane momenta. The effective mass at the zone center shows large variations of up to a factor of 7, and in one instance, the sign of the effective mass is reversed. These anomalous results are explained in terms of the bulk band structures of Pb and Si and an anticrossing coupling.

DOI: 10.1103/PhysRevB.71.033403

PACS number(s): 68.55.Jk, 73.21.Fg, 79.60.Dp

Unusual electronic features emerge as the dimensions of solids are decreased.<sup>1</sup> In thin films deposited on substrates, quantum-well states or subbands can arise from electrons confined in the films between the substrate and the vacuum.<sup>2–8</sup> Various quantum properties of such films have been investigated. The in-plane subband dispersion is of special interest, as it is related to charge transport and ballistic effects relevant to scientific and device applications in the quantum regime. Subband dispersion is usually free-electron-like near the zone center due to symmetry, and is often discussed in terms of an effective mass. The present work is a detailed examination of the dispersion in a simple model system, Pb films deposited on Si(111), which can be made with atomic uniformity. Such highly perfect films exhibit well-defined quantum-well states with a large lateral coherence length, thus permitting dispersion measurements over an unusually wide range of momentum. The results show both a case of sign reversal in effective mass and clear evidence of dramatic departure from parabolic dispersion. Specifically, near the surface Brillouin zone center all subbands, except one, disperse upward toward the Fermi level with increasing in-plane momentum. At larger in-plane momenta, all subbands turn sharply downward. While the overall gross features of the measurements can be explained by the Pb band structure alone, significant differences exist, including the magnitude and sign of the zone-center effective mass. These differences can be attributed to boundary effects including an anticrossing coupling between the Pb and Si states.

The experiment was performed at the Synchrotron Radiation Center, University of Wisconsin—Madison. A Si(111)-(7×7) surface was created; subsequently approximately 0.4 monolayers (ML) of Pb was deposited on the surface. The evaporation of Pb was performed by electron-beam heating of a tungsten crucible containing Pb, and the rate was monitored by a quartz microbalance. The sample was then annealed at  $\sim 700$  K to desorb the Pb to yield the Pb-terminated ( $\sqrt{3}\times\sqrt{3}$ )R30°- $\beta$  phase at a Pb coverage of 1/3 ML (in substrate units).<sup>9–11</sup> Further deposition of Pb on this surface at 100 K yielded atomically uniform films, as evidenced by the discrete evolution of quantum-well states

associated with the completion of each atomic layer.<sup>2</sup> The film thicknesses indicated below are the total number of full Pb monolayers in the film. The photoemission spectra were taken using a Scienta analyzer equipped with a two-dimensional detector with the sample at 100 K. A photon energy of 23 eV was used, except for the 5 and 6 ML films for which 29 and 24 eV photons were used, respectively. The analyzer recorded data over an angular span of 5.7°. To access points with a large in-plane momentum, the sample was rotated relative to the analyzer in steps of 4° to yield overlapping data sets. The light had an incident angle of 60° for normal emission, and was *p* polarized with the in-plane component of the polarization oriented along  $\bar{\Gamma}\bar{K}$ . The dispersion was measured along the  $\bar{\Gamma}\bar{K}$  direction.

The spectra for a film of thickness 7 ML as a function of the emission angle  $\theta$  relative to the surface normal are shown in Fig. 1. Figure 2(a) displays the data using gray (color) scales to represent the photoemission intensity as a function of the binding energy (vertical axis) and the emission angle  $\theta$  (horizontal axis). Four dispersive subbands are clearly seen, and the peak positions deduced from a fit are highlighted in Fig. 2(b). Near the zone center ( $\theta=0$ ), only one peak is visible. Its dispersion as a function of emission angle relative to the surface normal is symmetrically parabolic with a positive effective mass. This type of parabolic behavior has been reported before for several systems.<sup>12–17</sup> However, as the emission angle reaches beyond  $\sim 13^\circ$ , the peak turns around sharply toward higher binding energies. Such drastic departure from parabolic dispersion has never been reported before. One reason is that subbands in thin films can be difficult to observe at large emission angles due to effects of film roughness and a finite in-plane coherence length.<sup>12,15</sup> In the present experiment, the films have a uniform thickness, and the effect of roughness is minimal. The peak, however, becomes much broader and weaker as it moves toward higher binding energies. A reason for this broadening is that, at higher binding energies outside the Si band gap, the Pb valence electrons are not fully confined. Coupling to the substrate continuum states leads to decay and a short lifetime. This also explains why only one intense quantum-well peak is seen at the zone center in Fig. 2(a) even though more are

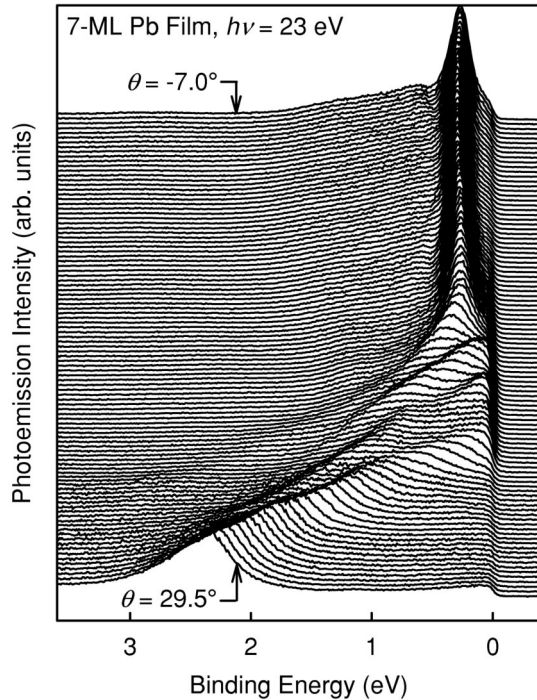


FIG. 1. Photoemission spectra for a 7 ML film taken at evenly spaced emission angles with a photon energy of 23 eV. The bottom curve is for  $\theta=29.5^\circ$  and the top curve is for  $\theta=-7.0^\circ$ .

predicted. This state is truly confined, as it is located above the Si valence-band maximum at  $\sim 0.5$  eV (corresponding to an  $n$ -type Schottky barrier height of 0.7 eV).<sup>18–20</sup> The other three subbands in Fig. 2(a) are derived from the same bulk band, but correspond to different quantum numbers. A careful inspection of Figs. 1 and 2 reveals additional weak and broad features, which could be due to resonances, higher-order processes, and minor sample imperfections, but these features are too indistinct for definitive assignment.

The subband dispersion is governed by the Bohr-Sommerfeld quantization rule

$$2k_{\perp}Nt + \Phi = 2n\pi, \quad (1)$$

where  $k_{\perp}$  is the perpendicular component of the electron momentum,  $N$  is the number of monolayers in the film,  $t$  is the monolayer thickness,  $\Phi$  is the total boundary phase shift, and  $n$  is a quantum number. The parallel component of the electron momentum  $k_{\parallel}$  is not quantized.  $\Phi$  is generally a function of both  $k_{\perp}$  and  $k_{\parallel}$ . If  $\Phi$  is known, one can determine from Eq. (1) the allowed values of  $k_{\perp}$  in terms of  $k_{\parallel}$  and  $n$ . The bulk band structure is thus reduced to a set of subbands  $E_n(k_{\parallel})$ . Figure 2(c) shows the expected subband dispersion relations based on this analysis using a tight-binding description of a first-principles calculation of the bulk band structure of Pb.<sup>21</sup> For simplicity, the phase shift  $\Phi$  is taken to be a constant chosen to match the model calculation to the experimental band at the zone center. The bulk band of interest here is the second lowest valence band, with the lowest band being the fully occupied  $s$  band at much higher binding energies. Each bulk band gives rise to seven subbands for a film thickness of 7 ML.

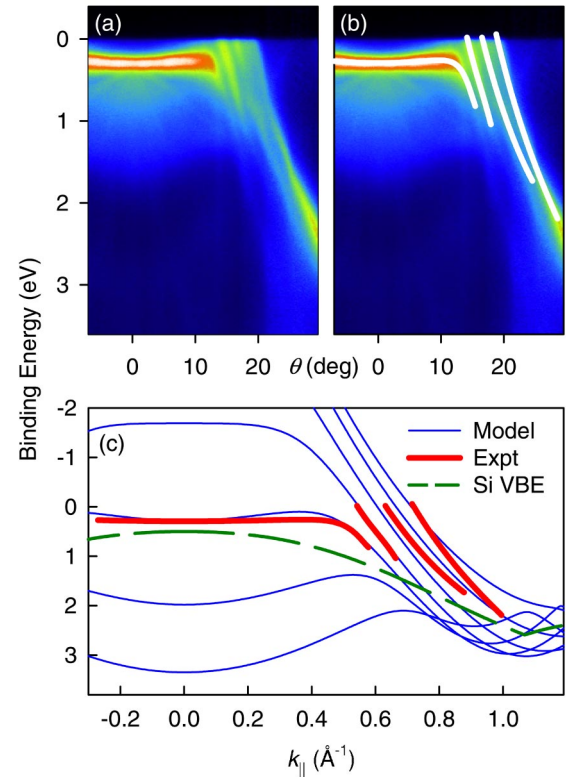


FIG. 2. (Color online) (a) The same data as in Fig. 1 presented using a gray (color) scale. The vertical axis is the binding energy, and the horizontal axis is the emission angle  $\theta$ . (b) The same with the subband dispersion relations highlighted. (c) Comparison of the experimental dispersion to the model calculation. The Si valence-band edge (VBE) is indicated by the dashed curve.

Also shown in Fig. 2(c), for comparison, are the experimental dispersion curves with the emission angle  $\theta$  converted to  $k_{\parallel}$ . The overall similarity demonstrates that the non-parabolic dispersion is a band structure effect. The agreement is, however, far from perfect. The observed subband near the zone center has a dispersion relation significantly flatter than the model calculation. An evaluation of the curvature yields an experimental effective mass about seven times as large as the model calculation, a very dramatic effect. The dashed curve in Fig. 2(c) indicates the Si valence-band edge, corresponding to the lower edge of confinement. All of the intense quantum-well emission features appear above this curve.

Figure 3 shows similar results obtained for a film with a thickness of 5 ML. There are just five subbands, and their dispersions are substantially different from the 7 ML case. As seen in the figure, all five subbands are observed experimentally over various ranges in  $k_{\parallel}$ . Near the zone center, the top subband's linewidth is relatively narrow. The subband below it is much broader because it is only partially confined. The phase shift  $\Phi$  is arbitrarily chosen to match this lower band at the zone center. It is interesting to note that the top subband has a negative curvature, or a negative effective mass, based on the experiment, while the model calculation shows a positive effective mass at the zone center. This sign reversal represents an even more dramatic departure from the

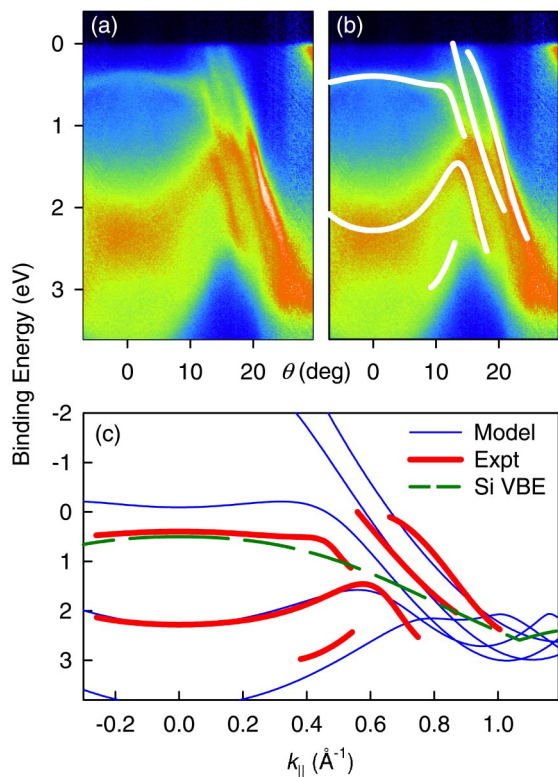


FIG. 3. (Color online) Same as Fig. 2, except the film thickness is 5 ML and the photon energy is 29 eV.

model calculation than the 7 ML case discussed above.

The subband effective mass has been the focus of a number of previous studies, and in some cases very large effective masses have been reported but never fully explained.<sup>12–14,16,17,21–23</sup> Our results indicate that indeed the subband dispersion can flatten to yield a very large effective mass, and in extreme cases, the curvature can even reverse to yield a sign change. By implication, the effective mass should diverge just at the verge of sign reversal. Since the subband dispersion is highly nonparabolic away from the zone center, care must be exercised in extracting the effective mass from the measurements. The experimental dispersion relations in Figs. 2 and 3 are deduced from a fit to the data. Near the zone center, the fit is done along the vertical direction for each energy distribution curve (EDC). Away from the zone center where the dispersion is almost vertical, the peak in an EDC can be extremely wide. The fit is performed instead in the horizontal direction for each momentum distribution curve. The resulting dispersion curve is numerically differentiated to yield the effective mass. The results for various film thicknesses  $N$  are summarized in Fig. 4. Also shown are results from two calculations, one based on the bulk band structure of Pb assuming a constant  $\Phi$ ,<sup>21</sup> and the other based on a slab calculation for free-standing Pb films without a substrate.<sup>3</sup> The two are fairly close, and the differences can be attributed to the effect of  $\Phi$  at the film-vacuum interfaces included in the slab calculation. Most of the data points in Fig. 4 agree fairly well with these calculations, but large differences, including a sign reversal, are seen for two data

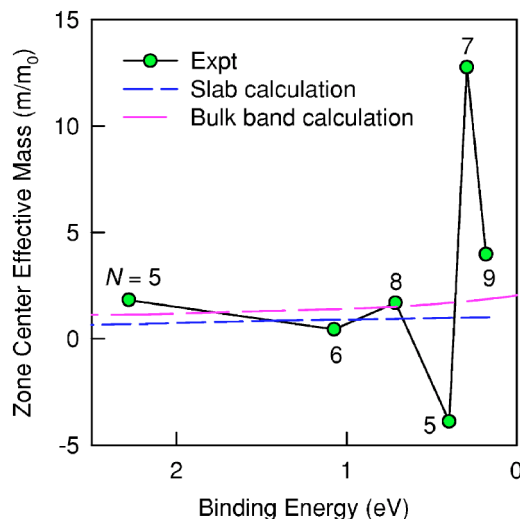


FIG. 4. (Color online) Subband effective mass  $m$  at the zone center as a function of binding energy, normalized to the free-electron mass  $m_0$ . The dots are experimental results, and the corresponding film thickness  $N$  is indicated. The two curves represent calculations based on the models discussed in the text. A photon energy of 23 eV was used, except for 5 and 6 ML films where 29 and 24 eV photons were used, respectively.

points, which correspond to the 7 and 5 ML cases discussed above.

An inspection of Figs. 2(c) and 3(c) reveals the origin of the large discrepancy in effective mass. In Fig. 3(c), the portion of the upper subband dispersion around the zone center nearly grazes the Si valence-band edge (the dashed curve). It appears as if the subband dispersion would dip below the Si valence-band edge, but could not do so due to a mutually repulsive interaction. This is, in fact, the case, and is just the usual anticrossing phenomenon familiar from quantum chemistry and atomic physics calculations. In essence, electronic coupling between states generally leads to an effective repulsion to avoid level crossings. The Si band gap itself is an example of anticrossing, although it is usually not described in these terms. In the present case, the Si substrate band edge is a robust electronic feature, independent of the overlayer configuration. The overlayer state tends to avoid it. The result is a subband nearly grazing the Si valence-band edge. The 7 ML case, shown in Fig. 2(c), is similar but less dramatic. The subband lies farther away from the Si valence-band edge. Nevertheless, the portion of the dispersion near the zone center appears to be pushed up by the repulsive interaction, resulting in a significant enhancement of the effective mass, but not a sign reversal. As expected, Fig. 4 shows that large deviations of the effective mass occur only near the Si valence-band maximum.

The changes in effective mass can also be discussed in terms of the phase shift. In Figs. 2(c) and 3(c), the energy differences between the model and the experimental dispersions are much smaller than the differences between one subband and the next. From Eq. (1), a variation in  $\Phi$  by  $2\pi$  is equivalent to changing the quantum number  $n$  by 1, and is thus equivalent to going from one subband to the next in

Figs. 2(c) and 3(c). In this sense, the differences between experiment and model are not large, and can be explained by a variation in  $\Phi$  by amounts substantially less than  $2\pi$ . Generally, the phase shift undergoes rapid changes (a van Hove-like singularity) just above the confinement edge,<sup>12,24,25</sup> and such rapid changes can account for the large variations in effective mass near the Si valence-band maximum.

In summary, in-plane dispersion of quantum-well subbands is an important and basic property for characterizing the electronic structure of films, but film imperfections can severely limit the measurements. Atomically uniform films of Pb on Si represent an excellent model system permitting a systematic investigation of the subband dispersion relation over a wide range of momentum. Unusual, nonparabolic shapes are observed that can be explained by bulk band structure effects. Large variations in effective mass, including a sign reversal, can be linked to boundary effects in terms

of an anticrossing coupling and phase shift. The work illustrates the connection of electronics in the nanoscale regime to the bulk and interfacial properties.

This work is supported by the U.S. National Science Foundation (Grant No. DMR-02-03003). We acknowledge the Petroleum Research Fund, administered by the American Chemical Society, and the U.S. Department of Energy, Division of Materials Sciences (Grant No. DEFG02-91ER45439), for partial support of the synchrotron beamline operation and the central facilities of the Frederick Seitz Materials Research Laboratory. The Synchrotron Radiation Center of the University of Wisconsin—Madison is supported by the U.S. National Science Foundation (Grant No. DMR-00-84402). The tight-binding code used for data analysis was provided by M. J. Mehl of the Naval Research Laboratory under the U.S. Department of Defense CHSSI program.

- 
- <sup>1</sup>T.-C. Chiang, Surf. Sci. Rep. **39**, 181 (2000).  
<sup>2</sup>J. J. Paggel, T. Miller, and T.-C. Chiang, Science **283**, 1709 (1999).  
<sup>3</sup>A. Mans, J. H. Dil, A. R. H. F. Ettema, and H. H. Weitering, Phys. Rev. B **66**, 195410 (2002).  
<sup>4</sup>M. Jalochoski, H. Knoppe, G. Lilienkamp, and E. Bauer, Phys. Rev. B **46**, 4693 (1992).  
<sup>5</sup>M. Jalochoski, M. Hoffmann, and E. Bauer, Phys. Rev. B **51**, 7231 (1995).  
<sup>6</sup>Th. Schmidt and E. Bauer, Surf. Sci. **480**, 137 (2001).  
<sup>7</sup>S. Stepanovskyy, V. Yeh, M. Hupalo, and M. C. Tringides, Surf. Sci. **515**, 187 (2002).  
<sup>8</sup>M. Hupalo, V. Yeh, L. Berbil-Baustista, S. Kremmer, E. Abram, and M. C. Tringides, Phys. Rev. B **64**, 155307 (2001).  
<sup>9</sup>I.-S. Hwang, R. E. Martinez, C. Liu, and J. A. Golovchenko, Surf. Sci. **323**, 241 (1995).  
<sup>10</sup>J. A. Carlisle, T. Miller, and T.-C. Chiang, Phys. Rev. B **45**, 3400 (1992).  
<sup>11</sup>P. J. Estrup and J. Morrison, Surf. Sci. **2**, 465 (1964).  
<sup>12</sup>M. A. Mueller, A. Samsavar, T. Miller, and T.-C. Chiang, Phys. Rev. B **40**, 5845 (1989).  
<sup>13</sup>M. A. Mueller, T. Miller, and T.-C. Chiang, Phys. Rev. B **41**, 5214 (1990).  
<sup>14</sup>P. D. Johnson, K. Garrison, Q. Dong, N. V. Smith, Dongqi Li, J. Mattson, J. Pearson, and S. D. Bader, Phys. Rev. B **50**, 8954 (1994).  
<sup>15</sup>L. Aballe, C. Rogero, P. Kratzer, S. Gokhale, and K. Horn, Phys. Rev. Lett. **87**, 156801 (2001).  
<sup>16</sup>F. G. Curti, A. Danese, and R. A. Bartynski, Phys. Rev. Lett. **80**, 2213 (1998).  
<sup>17</sup>Iwao Matsuda, Toshiaki Ohta, and Han Woong Yeom, Phys. Rev. B **65**, 085327 (2002).  
<sup>18</sup>D. R. Heslinga, H. H. Weitering, D. P. van der Werf, T. M. Klapwijk, and T. Hibma, Phys. Rev. Lett. **64**, 1589 (1990).  
<sup>19</sup>R. F. Schmitsdorf and W. Mönch, Eur. Phys. J. B **7**, 457 (1999).  
<sup>20</sup>M. H. Upton, C. M. Wei, M. Y. Chou, T. Miller, and T.-C. Chiang, Phys. Rev. Lett. **93**, 026802 (2004), and unpublished.  
<sup>21</sup>D. A. Papconstantopolous, *Handbook of the Band Structure of Elemental Solids* (Plenum Press, New York, 1986).  
<sup>22</sup>A. Danese, D. A. Arena, and R. A. Bartynski, Prog. Surf. Sci. **67**, 249 (2001).  
<sup>23</sup>Y. Z. Wu, C. Y. Won, E. Rotenberg, H. W. Zhao, F. Toyoma, N. V. Smith, and Z. Q. Qiu, Phys. Rev. B **66**, 245418 (2002).  
<sup>24</sup>N. V. Smith, Phys. Rev. B **32**, 3549 (1985).  
<sup>25</sup>C. M. Wei and M. Y. Chou, Phys. Rev. B **66**, 233408 (2002).